



This open access document is posted as a preprint in the Beilstein Archives at <https://doi.org/10.3762/bxiv.2021.70.v1> and is considered to be an early communication for feedback before peer review. Before citing this document, please check if a final, peer-reviewed version has been published.

This document is not formatted, has not undergone copyediting or typesetting, and may contain errors, unsubstantiated scientific claims or preliminary data.

Preprint Title Study on the Interaction Between Melamine-Cored Schiff Bases with Cucurbit[*n*]urils of Different Sizes and Its Application in Detecting Silver Ion

Authors Jun-Xian Gou, yang luo, Xi-Nan Yang, Wei Zhang, Ji-Hong Lu, Zhu Tao and xin xiao

Publication Date 29 Sep 2021

Article Type Full Research Paper

Supporting Information File 1 Supporting Information-GJX.docx; 4.9 MB

ORCID® iDs xin xiao - <https://orcid.org/0000-0001-6432-2875>

Study on the Interaction Between Melamine-Cored Schiff Bases with Cucurbit[*n*]urils of Different Sizes and Its Application in Detecting Silver Ion

Jun-Xian Gou[†], Yang Luo^{*†}, Xi-Nan Yang, Wei Zhang, Ji-Hong Lu, Zhu Tao, Xin Xiao^{*}

Key Laboratory of Macrocyclic and Supramolecular Chemistry of Guizhou Province, Guizhou University, Guiyang 550025, China.

Email: Xin Xiao - gyhxxiaoxin@163.com

* Corresponding author: gyhxxiaoxin@163.com (Xin Xiao), ouyyangl@126.com (Yang Luo)

[†] joint first author

Abstract

Three different complexes, TMeQ[6]-TBT, Q[7]-TBT and Q[8]-TBT, are constructed by three different cucurbiturils and synthesized guest melamine-cored Schiff base (TBT) through outer-surface interaction and host-guest interaction, where TBT and TMeQ[6] form complex TMeQ[6]-TBT through outer-surface interaction, while TBT and Q[7,8] form complexes Q[7]-TBT and Q[8]-TBT through host-guest interaction., and finally, Q[7]-TBT is selected as a UV detector for the detection of precious metal Ag⁺. This work makes full use of the characteristics of each cucurbiturils and combines that of Schiff bases to construct a series of complexes and apply them to metal detection.

Keywords

Melamine; cucurbiturils; Schiff base; Ag⁺

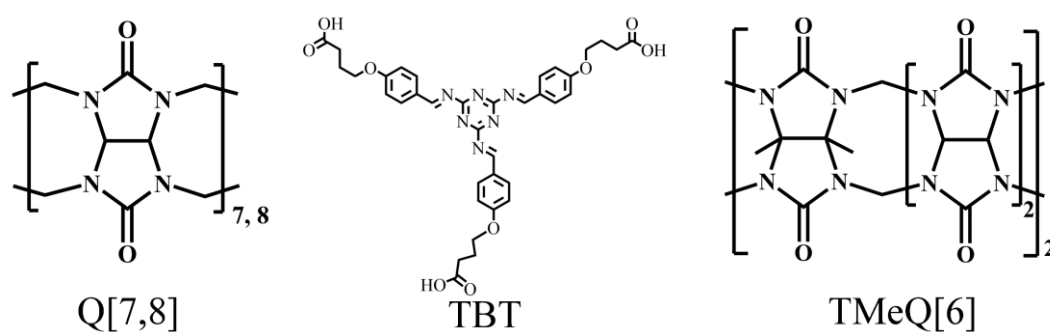
Introduction

Schiff bases ^[1], usually synthesized by the condensation of ammonia and active carbonyl compound, endowing them both hard nitrogen and oxygen donor atoms ^[2-5], are not only readily coordinate with various transition metal ions to yield different metal-organic framework ^[6-11], but also can be used as analytical reagents for the detection of different organic and inorganic substances ^[12-14].

Cucurbit[n]urils (Q[n]s, Scheme 1), a kind of supramolecular compound, formed by polymerization of glycoluril, contain rigid cavity for the study of host-guest chemistry and carbonyl groups for the study of coordination chemistry ^[15-19]. For the special methyl cucurbit[n]urils endowed with abundant methyl groups, its high density of the electropositivity can be used to study of outer-surface interaction of cucurbit[n]urils ^[20-23].

In this work, nitrogen-rich melamine is used as the center to synthesize the Schiff bases TBT through the Schiff base reaction and the nucleophilic reaction of haloalkane (Scheme 1 and S1) ^[24]. On the basis of retaining the abundant coordination sites of Schiff bases, TBT also modified with the carbon chain of appropriate length as the site of host-guest interaction and carboxyl group is used as the site of the outer-surface interaction. Then three kinds of cucurbit[n]urils with different size of cavities are chosen, tetramethylcucurbit[6]uril (TMeQ[6]), Q[7] and Q[8], to study their interaction with TBT ^[25-30]. Due to the small cavity size and the higher density of positive charge of TMeQ[6], TBT cannot enter the cavity of TMeQ[6], and instead has an outer-surface interaction with the exposed methyl group of it on the outer surface. The cavity of Q[7]

is just right for the carbon chain of TBT, so TBT can have host-guest interactions with Q[7]. With the addition of Q[8] with larger cavity into TBT, a supermolecule polymer Q[8]-TBT is constructed. Since Q[7] and TBT constitute a host-guest complex, the carboxyl group at the end of TBT and the carbonyl group of the Q[7] still have a strong ability to coordinate with metals. Therefore, Q[7]-TBT is selected for the detection of precious metal Ag^+ .



Scheme 1 The Structure of Q[7], Q[8], TMeQ[6] and TBT.

Results and Discussion

The outer-surface interaction of TMeQ[6]-TBT

In order to investigate the outer-surface interaction between TMeQ[6] and TBT, ^1H NMR titration is used. As shown in Figure 1, with the addition of TMeQ[6], the proton signal peak is shifted accordingly. For example, the signal of both H_a , H_b and H_c are shifted downfield, while the signal of H_d , H_e and H_f have almost unchanged in the presence of TMeQ[6]. Therefore, it can be preliminarily inferred that the interaction between TMeQ[6] and TBT is mainly driven by outer-surface interaction between the carboxylic carbon chain of TBT and the methyl or hydrogen of TMeQ[6] on its outer surface. In addition, when using UV-vis spectrum (Figure S5 and S6) to investigate the interaction between them, it is found that the presence of TMeQ[6] did not affect the

absorbance of TBT, which infers that TMeQ[6] does not interact with the benzene ring or the melamine of TBT. On the contrary, their outer-surface interaction occurs on the outer surface of TMeQ[6] and the carboxyl group of TBT, which is consistent with the results of NMR.

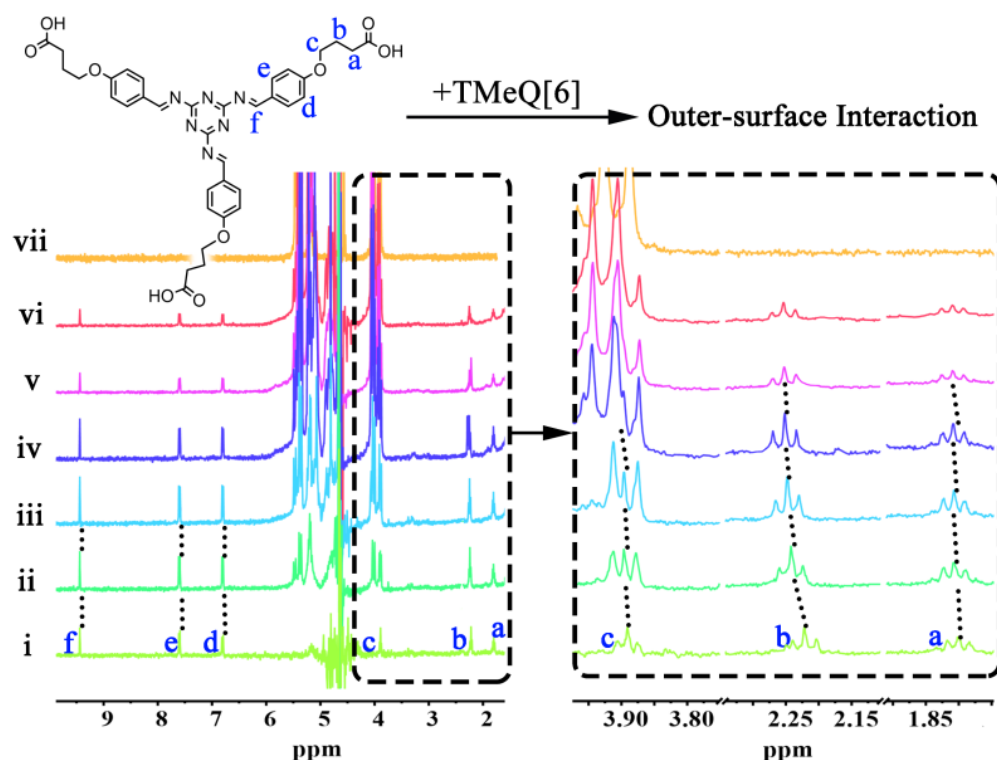


Figure 1 The ^1H NMR titration of TBT (1 mM) with an increasing amount of TMeQ[6] from 0 (i), 0.1 (ii), 0.2 (iii), 0.6 (iv), 1.0 (v) to 1.4 (vi). And the ^1H NMR of free TMeQ[6] (vii) in D_2O .

The host-guest interaction of Q[7]-TBT

Using the same ^1H NMR titration method as above to investigate the interaction between Q[7] and TBT, it is found that their interaction changes significantly, from the outer-surface interaction to host-guest interaction because of the larger cavity of Q[7]. As shown in Figure 2, the proton signal peak of the entire TBT upfield with the increasing amount of Q[7]. For example, the signal of H_a shifted from $\delta = 1.88$ ppm to

1.64 ppm, H_b from δ = 2.32 ppm to 2.25 ppm, H_c from δ = 3.97 ppm to 3.34 ppm, H_d from δ = 6.88 ppm to 5.87 ppm, H_e from δ = 7.68 ppm to 7.06 ppm and H_f from δ = 9.52 ppm to 9.29 ppm. Naturally, it can be inferred that Q[7] bound with the entire TBT with a strong host-guest interaction.

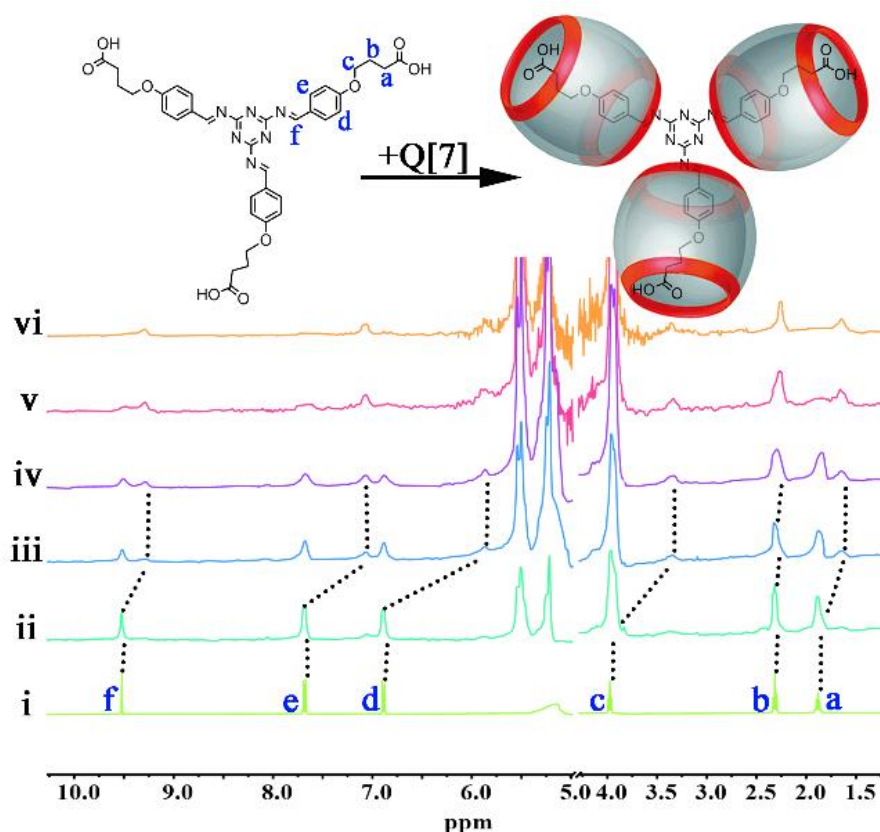


Figure 2 The ¹H NMR titration of TBT (1 mM) with an increasing amount of Q[7] from 0 (i), 0.1 (ii), 0.5 (iii), 1.0 (iv), 2.0 (v) to 3.0 (vi) in D₂O.

In addition, we also used UV-vis spectrum to verify above inference and further investigate their molar ratio in detail. Q[7] has a larger cavity compared with TMeQ[6], that can bind with TBT, so the absorbance of TBT gradually decreases and redshifts in the presence of Q[7] (Figure 3), which is mainly due to the π - π^* and n - π^* transition caused by the hydrophobic effect of the Q[7] cavity after binding with the phenyl and carboxyl groups of TBT. Meanwhile, the absorbance of TBT is gradually approaching the saturation state, when the amount of Q[7] reaches 3 times the amount of TBT.

Therefore, it can be inferred that Q[7] binds with the three “arms” of TBT at a molar ratio of 3:1 ($N_{Q[7]}:N_{TBT} = 3:1$) and forms a host-guest complex Q[7]-TBT. In addition, the ITC experiment also strongly supports the above results, which data can be fitted to a very suitable curve using the model of Sequential Three Site (Figure S7), and corresponding binding ability (K_a) is $1.422 \times 10^6 \text{ M}^{-1}$.

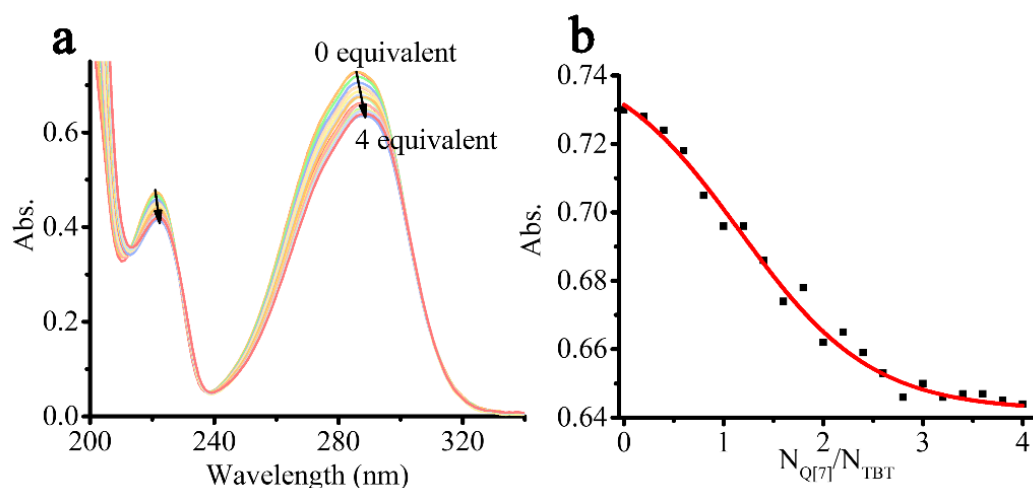


Figure 3 The UV-vis spectra (a) of TBT (20 μM) with an increasing amount of Q[7] from 0.0 to 4.0; the plots (b) of $N_{Q[7]}/N_{TBT}$ vs. absorbance of TBT in water at $\lambda=286 \text{ nm}$.

The host-guest interaction of Q[8]-TBT

Since Q[8] has a larger cavity than Q[7], it can definitely bind the entire TBT molecule like Q[7]. However, in the ^1H NMR titration experiment (Figure S8), it's found that upon the addition of Q[8], the chemical shift value of TBT did not change significantly. But with the continuous increase concentration of Q[8], the proton signal of TBT began to weaken and the proton signal of Q[8] has not been detected during the whole experiment. In addition, UV-vis spectrum in Figure 4a shows that, as continuously increasing amount of Q[8], the absorbance of TBT keeps on decrease from $A= 0.735$ to 0.112 ($\Delta A=0.623$), and is no red shift or blue shift. Both of above phenomena and experiment show that Q[8] interacted with the “arm” of TBT and produced

corresponding precipitation due to aggregation, which is also the reason why the proton signal and absorbance of TBT in the ^1H NMR and UV-vis spectra have been greatly reduced. Then SEM and Dynamic Light Scattering (DLS) are used for in-depth research of Q[8]-TBT complex. As shown in Figure 4b, compared with the particle size of TBT (5.35 nm), the particle size of Q[8]-TBT is greatly increased to 3726.58 nm, while SEM (Figure S10) also observed a large number of massive Q[8]-TBT complex.

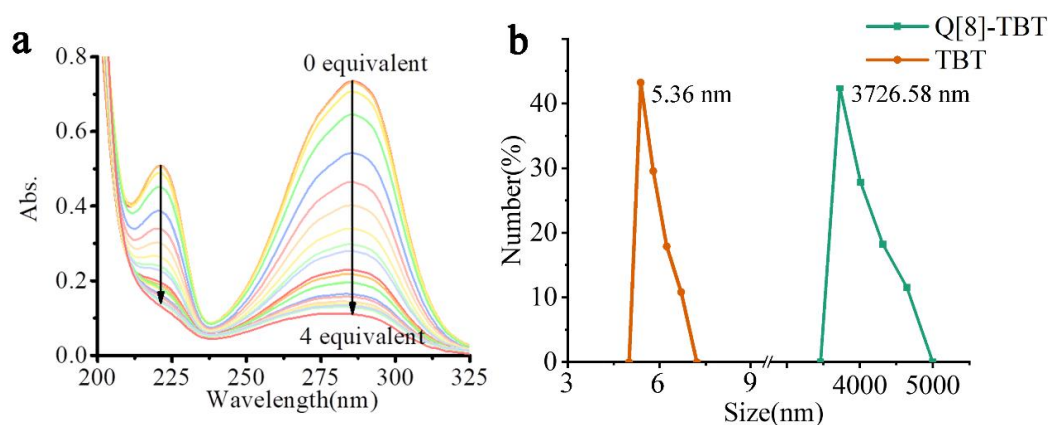


Figure 4 The UV-vis spectra (a) of TBT (20 μM) with an increasing amount of Q[8] from 0.0 to 4.0 and the DLS of TBT(20 μM) and Q[8]-TBT(3:1, 20 μM).

Detection of Ag^+ based on Q[7]-TBT

The guest molecule TBT contains three carboxyl groups and a wealth of lone-pair electrons, so it has a high binding ability to metals. In this study, Q[7]-TBT was selected as a UV detector to detect common metals. As shown in Figure 5, the additional Ag^+ increases the absorbance of the Q[7]-TBT complex from 0.441 to 0.555 at $\lambda_{\text{max}}=258$ nm, while other metal ions do not increase or decrease significantly at this wavelength, so Q[7]-TBT have a higher selectivity to Ag^+ among metals. In addition, in the anti-interference experiment, Q[7]-TBT also has a good performance in the detection of silver ions in the presence of other common metals.

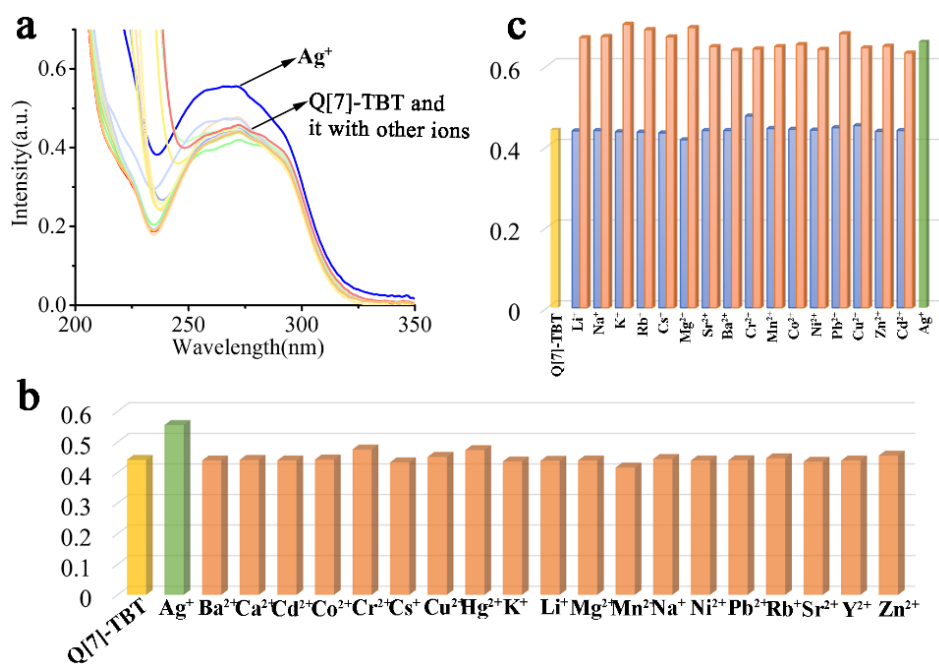


Figure 5 The UV-vis spectra (a) of Q[7]-TBT (3:1, 20 μM) affected by Mⁿ⁺ (50 equivalents); Histogram of (b) Q[7]-TBT in the presence of Mⁿ⁺ and (c) the anti-interference experiment.

In order to further explore the detection limit (DL) and detection mechanism of Q[7]-TBT towards Ag⁺, UV-vis titration experiment was carried out. As shown in Figure 6, with the continuous addition of Ag⁺, the absorbance of Q[7]-TBT continues to increase at $\lambda_{\max}=258$ nm, which is caused by the n- π^* transition of Q[7]-TBT. Therefore, it can be further inferred that Ag⁺ mainly binds with the carboxyl group of TBT. In addition, we calculated the value of DL is 3.91×10^{-6} M, and the corresponding fitting formula is $y = -0.01 + 0.0182x$ with a high $R^2 = 0.997$.

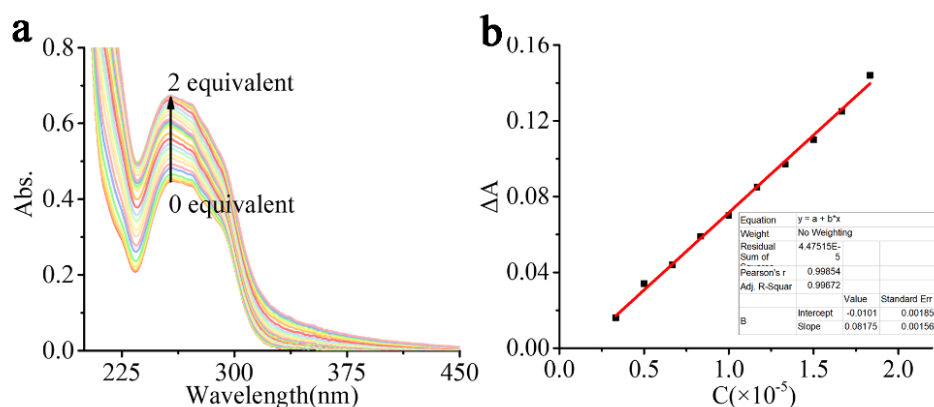
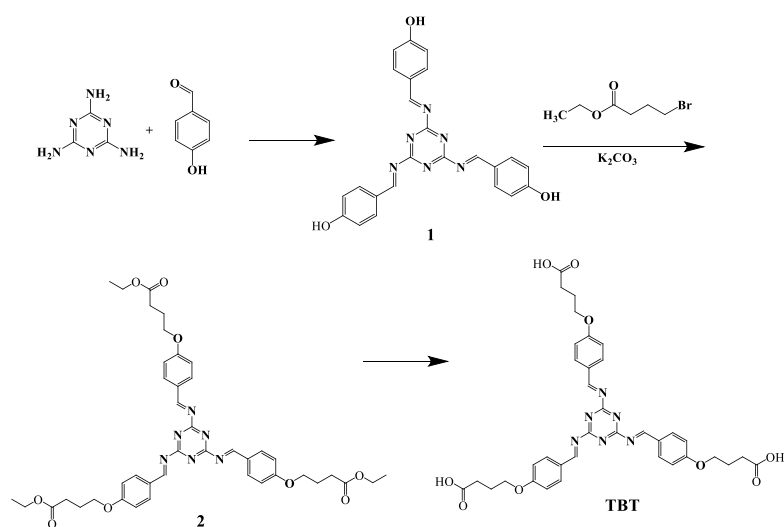


Figure 6 The UV-vis spectra (a) of Q[7]-TBT (20 μ M) with an increasing amount of Ag^+ from 0.0 to 2.0; DL plot (b) of Ag^+ .

Conclusion

Three different complexes, TMeQ[6]-TBT, Q[7]-TBT and Q[8]-TBT, are constructed from three different cucurbiturils with the same molecule TBT. Due to the subtle attribute gap between cucurbiturils, TMeQ[6]-TBT complex is driven by outer-surface interaction, Q[7]-TBT and Q[8]-TBT complex are formed by host-guest interaction. Finally, Q[7]-TBT is selected as a UV detector for the detection of precious metal Ag^+ . This work fully demonstrates the charm of the rigid cavity of cucurbiturils. Different cucurbiturils can selectively bind guest molecules in the different way according to their own characteristics. In addition, the Q[7]-TBT complex constructed in this paper combines with the advantage of the strong coordination ability of melamine core Schiff base, and is applied to metal detection, providing a theoretical study for the Q[*n*]-Schiff base complex.

Experimental



Scheme 2 The synthesis routes of TBT.

The synthesis of 1: Melamine (10 mmol, 1.26 g) was suspended in benzene (20 mL) and a suspension of 4-hydroxybenzaldehyde (30 mmol, 3.66 g) in benzene (30 mL) was added by stirring, then reflux overnight. The pink powder was formed and washed with warm water to get the pure compound 1. 1H NMR in $DMSO-d_6$: $\delta=$ 12.1 ppm (s,3H), $\delta=$ 9.76 ppm (s,3H), $\delta=$ 7.80 ppm (d, 6H), $\delta=$ 7.08 ppm (d, 6H), $\delta=$ 4.06 ppm (t, 6H), $\delta=$ 2.40 ppm (t, 6H), $\delta=$ 1.93 ppm (m, 6H).

The synthesis of 2: K_2CO_3 (0.138 g, 1.0 mmol) and compound 1 (0.438 g, 1.0 mmol) were dissolved into acetonitrile (80 mL) and refluxed for 3hs. Ethyl 4-bromobutyrate (0.918 g, 3 mmol) was added and refluxed for a day. The solvent is removed, and then separated by column chromatography (EA/PE) to get the pure compound 2. 1H NMR in $DMSO-d_6$: $\delta=$ 9.82 ppm (s,3H), $\delta=$ 7.82 ppm (d,6H), $\delta=$ 7.07 ppm (d, 6H), $\delta=$ 7.08 ppm (d, 6H), $\delta=$ 4.04 ppm (m, 14H), $\delta=$ 1.95 ppm (m, 9H), $\delta=$ 1.13 ppm (t, 12H).

The synthesis of TBT: compound 2 (0.780 g, 1.0 mmol) and NaOH (0.27 g, 6.75 mmol) were combined in a 1:1 solution of acetonitrile: water (20 mL) and reflux for 4hs. The mixture was concentrated under vacuum and then acidified it by HCl to pH=2 to

precipitate a white solid **TBT**. ¹H NMR in DMSO-d₆: δ= 12.23 ppm (s,3H), δ=9.90 ppm (s, 3H), δ= 7.81 ppm (d, 6H), δ= 7.08 ppm (d, 6H), δ= 4.05 ppm (t, 6H), δ= 2.35 ppm (t, 6H), δ=1.92 ppm (m, 6H).

Supporting Information

Supporting Information File 1:

File Name: Supporting Information-GJX

File Format: Microsoft Word

Title: Supporting Information

Funding

This work was supported by the National Natural Science Foundation of China (No. 21861011, 21871064) and the Innovation Program for High-level Talents of Guizhou Province (No. 2016-5657).

References

1. Schiff H. *Justus Liebigs Annalen der Chemie*, **1864**, 131, 118-119.
2. Jia Y., Li J. *Chemical Reviews*, **2015**, 115(3), 1597-1621.
3. Rezaeivala M., Keypour H. *Coordination Chemistry Reviews*, **2014**, 280(1), 203-253.
4. Horak E., Vianello R., Hranjec M., et al. *Supramolecular Chemistry*, **2018**, 30, 891-900.

5. Nastasă C., Vodnar D. C., Ionut I., et al. *Int. J. Mol. Sci.*, **2018**, *19*(1), 222.
6. Gupta K., Sutar A. K. *Coordin. Chem. Rev.*, **2008**, *252*, 1420-1450.
7. Aluthge D. C., Patrick B. O., Mehrkhodavandi P. *Chem. Commun.*, **2013**, *49*, 4295-4297.
8. Okuhata M., Funasako Y., Takahashi K., et al. *Chem. Commun.*, **2013**, *49*, 7662-7664.
9. Seo M.-S., Kim K., Kim H. *Chem. Commun.*, **2013**, *49*, 11623-11625.
10. Fu S., Liu Y., Ding Y., et al. *Chem. Commun.*, **2014**, *50*, 2167-2169.
11. Matsunaga S., Shibasaki M. *Chem. Commun.*, **2014**, *50*, 1044-1057.
12. Wang T., Douglass E. F., Fitzgerald K. J., et al. *J. Am. Chem. Soc.*, **2013**, *135*, 12429-12433.
13. Jinmin W. and Bing Y. *Anal. Chem.*, **2019**, *91*, *20*, 13183-13190.
14. Kevin J. B., Ryan R. W., Thomas F. B., et al. *J. Am. Chem. Soc.*, **2017**, *139*, *15*, 5338-5350.
15. W. A. Freeman, W. L. Mock, N. Y. Shih. *J. Am. Chem. Soc.*, **1981**, *103*, *24*, 7367-7368.
16. Jae Wook Lee, S. Samal, N. Selvapalam, Hee-Joon Kim, and Kimoon Kim. *Acc. Chem. Res.*, **2003**, *36*, *8*, 621-630.
17. Simin Liu, Peter Y. Zavalij, and Lyle Isaacs. *J. Am. Chem. Soc.*, **2005**, *127*, *48*, 16798-16799.
18. Xiran Yang, Fengbo Liu, Zhiyong Zhao, Feng Liang, Haijun Zhang, Simin Liu. *Chinese Chemical Letters*, **2018**, *29*, 1560-1566.
19. Guocan Yu, Kecheng Jie, and Feihe Huang. *Chem. Rev.*, **2015**, *115*, *15*, 7240-7303.
20. X. L. Ni, X. Xiao, Z. Tao and et al. *Acc. Chem. Res.*, **2014**, *47*, 1386.

21. Y. Huang, R. H. Gao, M. Liu, Z. Tao and et al. *Angew. Chem. Int. Ed.*, **2021**, *60*, 15166-15191.
22. Ming Liu, Lixia Chen, Peihui Shan, Chengjie lian, Zenghui Zhang, Yunqian Zhang, Zhu Tao and Xin Xiao. *ACS Appl. Mater. Inter.*, **2021**, *13*, 7434-7442.
23. Dan Yang, Ming Liu, Xin Xiao, Zhu Tao, Carl Redshaw. *Coordin. Chem. Rev.*, **2021**, *434*, 213733
24. Saban Uysal, Ziya Erdem Koc. *Journal of Hazardous Materials*, **2010**, *175*, 532-539.
25. Anna K.-A., Jonathan C. A., Selena H., Rafal M. D., et al. *J. Am. Chem. Soc.*, **2020**, *142*, 20513-20518.
26. Huang Wu, Yu Wang, Leighton O. Jones, et al. *J. Am. Chem. Soc.*, **2020**, *142*, 39, 16849-16860.
27. Zehuan Huang, Xiaoyi Chen, Guanglu Wu, et al. *RSC Adv.*, **2021**, *11*, 3470-3475.
28. Ye Meng, Weiwei Zhao, Jun Zheng, et al. *RSC Adv.*, **2021**, *11*, 3470-3475.
29. Shuang Li, Wen Xia, Yunqian Zhang, et al. *New J. Chem.*, **2020**, *44*, 11895-11900.
30. Weitao Xu, Xinyu Deng, Xin Xiao, et al. *New J. Chem.*, **2020**, *44*, 4311-4318.